RELATIONSHIP BETWEEN MEMBRANE EXCITABILITY AND SINGLE CHANNEL OPEN-CLOSE KINETICS

JOHN R. CLAY AND LOUIS J. DEFELICE
Laboratory of Biophysics, National Institute of Neurological, Communicative Disorders and Stroke, National Institutes of Health at the Marine Biological Laboratory, Woods Hole, Massachusetts 02543, and Department of Anatomy, Emory University, Atlanta, GA 30322

ABSTRACT We have developed a novel technique for simulating the influence of the effects of single channel kinetics on the voltage changes associated with membrane excitability. The technique uses probability distribution functions for the durations of channel open- and closed-state lifetimes, which can be calculated for any model of the ion conductance process. To illustrate the technique, we have used the Hodgkin and Huxley model of nerve membrane ion conductances to simulate channel kinetics during predetermined voltage changes, such as a voltage jump and an action potential. We have also simulated the influence of channels on voltage changes in a free running, non–voltage-clamped patch of membrane 1 μm^2 or less in area. The latter results provide a direct illustration of the relationship between fluctuations of membrane excitability and fluctuations in channel open- and closed-state lifetimes.

INTRODUCTION

Recent measurements with the patch voltage-clamp technique have demonstrated that ionic channels in excitable membranes have discrete open- and closed-conductance states, the durations of which are random variables (Conti and Neher, 1980; Sigworth and Neher, 1980). We have simulated the kinetics of the open-close process on a digital computer using a random number generator and the probability distribution functions of open- and closed-channel lifetimes. The distribution functions can be calculated for any model of the ionic conductance process from probability theory. These functions can be used to predict channel behavior for any voltage change, including changes that are caused by the channels themselves in the free-running, unclamped membrane. We have used this technique to simulate the kinetics of small populations of sodium and potassium channels during voltage-clamp steps and during an action potential using the Hodgkin and Huxley (1952) model of ionic conductances in nerve membrane. We have also determined the influence of individual channels on the excitability of small membrane patches 1 μm^2, or less, in area.

The technique that we describe in this paper provides a novel, straightforward way to predict ionic currents and patterns of excitability in the microscopic, single-channel domain from macroscopic equations of ion conductance.

METHODS

The Hodgkin and Huxley (1952) model is described by

$$C_M\, dV/dt + \bar{g}_K n^4 (V - E_K) + \bar{g}_{Na} m^3 h (V - E_{Na}) + \bar{g}_L (V - E_L) = I_{app} \quad (1)$$

where C_M and V are membrane capacitance and membrane potential, respectively; I_{app} is externally applied current; E_K, E_{Na}, and E_L are the equilibrium Nernst potentials for sodium, potassium and leakage ionic currents, respectively; $\bar{g}_K$, $\bar{g}_{Na}$, and $\bar{g}_L$ are the fully activated conductances for the respective ions; and n, and m, and h are first-order voltage- and time-dependent conductance parameters, which are described by $\dot{x} = dx/dt = -[\alpha_x(V) + \beta_x(V)]x + \alpha_x(V)$, where x is either h, m, or n. We take the resting potential to be -60 mV, and $E_K = -72$ mV, $E_{Na} = 55$ mV, $E_L = -49$ mV; $\alpha_n(V) = -0.01(V + 50)/\{\exp[-0.1(V + 50)] - 1\}$, $\beta_n(V) = 0.125 \exp[-(V + 60)/80]$; $\alpha_m(V) = -0.1(V + 35)/\{\exp[-0.1(V + 35)] - 1\}$; $\beta_m(V) = 4 \exp[-(V + 60)/18]$; $\alpha_h(V) = 0.07 \exp[-(V + 60)/20]$; $\beta_h(V) = 1/\{\exp[-0.1(V + 30)] + 1\}$, $C_M 1 = \mu F/cm^2$.

Noise measurements from nerve suggest that the potassium and sodium channel densities are 60 and 300 μm^{-2}, respectively (Conti et al., 1975). We used these estimates together with single-channel conductances $\gamma_K = 6$ pS and $\gamma_{Na} = 4$ pS so that our fully activated conductances were consistent with the Hodgkin and Huxley (1952) model values of $\bar{g}_K = 36$ mS·cm^{-2} and $\bar{g}_{Na} = 120$ mS·cm^{-2}. We assumed that leakage channels ($\bar{g}_L = 0.3$ mS·cm^{-2}) do not exhibit gating kinetics. The interpretation of the n^4 and m^3h processes that is consistent with the observation of open-close kinetics consists of assigning four independent open-close particles to each channel, all of which must be open for any given channel to be conducting (Hill and Chen, 1972; Stevens, 1972). Each potassium channel has four identical particles with a rate constant of $\alpha_n(V)$ for transition from closing to opening and $\beta_n(V)$ for the reverse transition. Similarly, each sodium channel has three identical particles with rate constants given by $\alpha_m(V)$ and $\beta_m(V)$, and a fourth particle (the inactivation process) with rate constants given by $\alpha_h(V)$ and $\beta_h(V)$. All rate constants are voltage dependent.

Voltage Jump Simulations

The above description of the gating process possesses the Markov property (Feller, 1971). That is, channels described by the Hodgkin and Huxley (1952) model lack memory of their previous history in voltage clamped conditions. Consequently, the probability distribution functions for the lifetimes of openings and closings of a gating particle are given by $P_o(T) = \exp[-\beta_x(V)T]$ and $P_c(T) = \exp[-\alpha_x(V)T]$, where $P_o(T)$, for example, is the probability that any single opening exceeds T, and x

represents either h, m, or n. We used these functions to analyze channel currents before and after a voltage jump from V_1 to V_2 (Fig. 1 *A* and 1 *B*). The time of occurrence of the jump was $t = t_j$. We assumed that the channels were initially ($t = 0$) in steady-state conditions, so the probability that any single gate was initially open was given by $p_o\ \alpha_x(V_1)/[\alpha_x(V_1) + \beta_x(V_1)]$. The initial condition of each particle was determined from p_o and a random number, r_1. All random numbers were uniformly distributed between 0 and 1. If $r_1 > p_o$, the particle was closed initially, and if $r_1 < p_o$, it was open initially. A second random number, r_2, was used to determine the lifetime of the initial condition. If a particle was initially closed, the duration of that closing was given by $T_c = -\alpha_x(V_1)^{-1}\log_e r_2$. The time $t = T_c$ marked the end of the initial closing and the beginning of the subsequent opening of the particle. The duration of the latter, T_o, was given by $T_o = -\beta_x(V_1)^{-1}\log_e r_3$. Succeeding closings and openings were determined in a similar manner until $t = t_j$, where the voltage changed from V_1 to V_2. Open- and closed-gating lifetimes subsequent to t_j were determined from $P_o(T)$ and $P_c(T)$ as above, with V_1 replaced by V_2, and from the initial conditions of each particle at $t = t_j$, as determined by the simulations up to that point in time. We note that $P_o(T)$ and $P_c(T)$ change instantaneously at $t = t_j$, as required by the Hodgkin and Huxley (1952) model. Throughout these simulations any single channel was assumed to be open only when all four gating particles were open.

Simulations for Continuous Predetermined Voltage Changes

The extension of the above analysis to conditions in which the membrane potential is continuously changing is not obvious, since the rate constants are parametric functions of time through their dependence on voltage, e.g., $\alpha_x(V) = \alpha_x[V(t)]$. Consider, for example, a continuous, predetermined voltage change, such as a voltage ramp, applied to a membrane in voltage-clamp conditions. During any single open- or closed-gating lifetime, the rate constants $\alpha_x(V)$ and $\beta_x(V)$ change continuously. Consequently, the above expressions for $P_o(T)$ and $P_c(T)$ are not applicable to this problem. It can be shown that the appropriate probability functions are given by (Karlin and Taylor, 1975)

$$P_o(T) = \exp\{-\int_0^T \beta_x[V(t)]\mathrm{d}t\}$$

and

$$P_c(T) = \exp\{-\int_0^T \alpha_x[V(t)]\mathrm{d}t\}. \quad (2)$$

That is, the duration of any single opening or closing is related to the average value of the appropriate rate constant during the lifetime in question. For example, consider a gating particle that is initially open at $t = 0$. We assign a random number, r_1, to the duration, T_o, of this initial condition, which can be determined from Eq. 2. The solution is

$$\int_0^{T_o} \beta_x[V(t)]\mathrm{d}t = -\log_e r_1. \quad (3)$$

The unknown in Eq. 3 is the limit of integration. All other terms in Eq. 3 are known a priori. At $t = T_o$, the particle closes. The duration of that closing, T_c, is determined from

$$\int_{T_o}^{T_o+T_c} \alpha_x(V(t)]\mathrm{d}t = -\log_e r_2, \quad (4)$$

where r_2 is the random number assigned to this closing. Because T_o has already been determined from Eq. 3, the only unknown in Eq. 4 is T_c. At $t = T_o + T_c$, the particle opens again. Succeeding lifetimes are determined in a similar manner.

We used the above analysis to simulate channel kinetics during the Hodgkin and Huxley (1952) model action potential assuming an initial condition of $V = -50$ mV (Fig. 1 *C* and *D*). We used $V = -50$ mV to determine the initial condition of gating particles in a manner similar to that used in the voltage-jump simulations. The action potential waveform was determined numerically from Eq. 1 using the Rush and Larsen (1978) integration technique with a time increment of 50 μs. This result was substituted for $V(t)$ in Eq. 2, as illustrated in Eqs. 3 and 4. The solutions to Eqs. 3 and 4 were determined numerically, using an Euler integration technique with a 50-μs time increment (Moore and Ramon, 1974). Separate simulations were carried out for each gating particle of each channel. As in the voltage-jump simulations, any single channel was assigned to its open state only when all four of its gating particles were open.

Simulations of Membrane Excitability

The above results provide the basis of our analysis for conditions in which the membrane is not voltage clamped. Our simulations for this problem concerned the influence of individual channels on voltage changes in small, unclamped membrane patches. We assigned specific values to each patch for capacitance C_s, from $C_M = 1\ \mu\mathrm{F\cdot cm^{-2}}$, and for channel numbers, N_K and N_{Na}, from the channel densities given above. Leakage current was set equal to zero. Changes both in V and in channel states subsequent to their initial conditions were determined from Eqs. 3 and 4 and from

$$C_s\mathrm{d}V/\mathrm{d}t + n_K\,\gamma_K\,(V - E_K) + n_{Na}\,\gamma_{Na}\,(V - E_{Na}) = I_{app} \quad (5)$$

where n_K and n_{Na} are the number of potassium and sodium channels, respectively, which are open during any given time interval. Specifically, the initial conditions for all gating particles and, consequently, n_K and n_{Na}, were determined as in the voltage-jump simulations, using the initial condition for membrane potential, $V(t = 0)$. Each channel particle was assigned a random number to be used to determine the duration of its initial condition. The voltage change, $V(t)$, subsequent to $t = 0$ was determined from Eq. 5. The initial lifetimes of all gating particles were determined from $V(t)$ and Eqs. 3 and 4. The results of this procedure were sequences of lifetimes, $T_{o,1}, T_{o,2}, \ldots T_{o,i}, \ldots T_{o,n_o}$; and $T_{c,1}, T_{c,2}, \ldots T_{c,i}, \ldots T_{c,n_c}$, where $T_{o,i}$ is the lifetime of the ith particle in the patch which was initially open, $T_{c,i}$ is the lifetime of the ith particle in the patch that was initially closed, n_o is the total number of particles that were initially open, and n_c is the total number of particles that were initially closed. Each channel in the patch is represented by four of these lifetimes. Any individual channel is open only when open time durations of all of its gating particles overlap. Consequently, $n_o + n_c = 4N_{Na} + 4N_K$. These sequences were searched for the minimum lifetime, be it either an opening or a closing. Assume, for example, that $T_{o,3}$ was the minimum of both sequences. At $t = T_{o,3}$ a particle in the patch closes, which may or may not cause the corresponding channel to change from its open to its closed conducting state. If the conductance state of the channel does not change, we assign a new random number to the particle in question, and we determine the duration of its subsequent closing from Eq. 4 and from $V(t)$. The result of this calculation is added to the sequence of particles that were initially closed, and $T_{o,3}$ is removed from the sequence of initial open durations. Both sequences are then searched for the time of occurrence of the next particle transition. This procedure is continued until the time, $t = t_1$, at which the first change of conductance of a channel occurs. The voltage change subsequent to t_1 is calculated from Eq. 5 with the appropriate modification of either n_K or n_{Na}. The lifetimes of all gating particles are also recalculated. For example, consider a particle whose initial lifetime was $T_{o,7}$ with $T_{o,7} > t_1$. Its new lifetime following t_1, $T'_{o,7}$, is now determined from Eq. 3 with the new $V(t)$ subsequent to t_1. As a further example, consider a particle whose initial lifetime was $T_{c,5}$, with $T_{c,5} < t_1$. Let its subsequent open duration be $T'_{o,5}$ with $T'_{o,5} > t_1 - T_{c,5}$. At $t = t_1$, the open duration is recalculated from Eq. 4 and $V(t)$ for $t > t_1$. Throughout these procedures Eqs. 3 and 4 were iterated numerically with 50 μs time increments. Eq. 5 was solved exactly to give $V(t)$ between each change of state of a channel. These simulations were continued in a manner similar to that of the voltage jump and the predetermined voltage change analyses. The primary difference between this analysis and the previous

cases is that $V(t)$ is not known, a priori. Moreover, the simulations must be carried out in parallel for all gating particles. The simulations in the previous cases were carried out in a serial manner. That is, a simulation was initiated and carried out to its conclusion separately for each gating particle.

Simulations for Other Models of Channel Gating

In recent years, alternative models for channel gating in nerve that differ in various ways from the original Hodgkin and Huxley (1952) model have been presented (Armstrong and Bezanilla, 1977; Armstrong and Gilly, 1979; Gilly and Armstrong, 1982). The extension of our analysis to these or other models is illustrated by considering an alternative interpretation of the Hodgkin and Huxley (1952) model. The Hodgkin and Huxley (1952) gating mechanism consists of four stochastically independent particles for each channel. Consequently, each different configuration of these open-close particles can be viewed as a state of the channel, with certain specified rates of transition to other configurational states. For example, a sodium channel can be represented by the state diagram (FitzHugh, 1965; Neher and Stevens, 1977)

$$\begin{array}{ccccccc} [0'] & \underset{\beta_m}{\overset{3\alpha_m}{\rightleftharpoons}} & [1'] & \underset{2\beta_m}{\overset{2\alpha_m}{\rightleftharpoons}} & [2'] & \underset{3\beta_m}{\overset{\alpha_m}{\rightleftharpoons}} & [3'] \\ \alpha_h \Big\| \beta_h & & \alpha_h \Big\| \beta_h & & \alpha_h \Big\| \beta_h & & \alpha_h \Big\| \beta_h \\ [0] & \underset{\beta_m}{\overset{3\alpha_m}{\rightleftharpoons}} & [1] & \underset{2\beta_m}{\overset{2\alpha_m}{\rightleftharpoons}} & [2] & \underset{3\beta_m}{\overset{\alpha_m}{\rightleftharpoons}} & [3] \end{array}$$

Diagram I

where the number inside each bracket in either the upper or lower tier of states represents the number of activation, or m gates, which are open in that particular state. The inactivation, or h gate, is open in the lower tier, and it is closed in the upper tier of states. Consequently, [3] is the open or conducting state of the channel. All other states have zero conductance. Alternative models for gating that have been described in the literature differ in detail but not in spirit from the above diagram. Some models have more than one conductance state; the topology of transitions between states in these models is generally different from that of Hodgkin and Huxley (1952); and the specific transition rates are generally different from the Hodgkin and Huxley (1952) α's and β's. Nevertheless, any state diagram can be represented by a set of first-order differential equations, as can the Hodgkin and Huxley (1952) model. The primary difference is that the equations for the gating of any single channel are generally coupled to each other in these alternative models, whereas the Hodgkin and Huxley (1952) model can be described by one equation for any single potassium channel and by two uncoupled equations for any single sodium channel.

The operational procedure for carrying out simulations with state diagrams differs somewhat from the analysis of the previous sections. Consider, for example, Diagram I above in steady-state voltage clamp conditions. The initial state that the channel occupies is determined from a random number, r_1, and the respective probabilities for each state, which are $h_\infty(1 - m_\infty)^3$, $3m_\infty(1 - m_\infty)^2h_\infty$, $3m_\infty^2(1 - m_\infty)h_\infty$, and $m_\infty^3h_\infty$ for states [0], [1], [2], and [3], respectively. The respective probabilities for states [0'], ... [3'] are similar with h_∞ replaced by $(1 - h_\infty)$. Each of these probabilities is assigned a portion of the real line between 0 and 1. The portion of the line on which r_1 lies determines the initial state. The duration of the initial state is determined from a second random number, r_2; the combined rate of transition for leaving that state to one or more of the other states; and the appropriate modification of the expressions for $P_o(T)$ and $P_c(T)$. For example, assume that the initial state was [2] in Diagram I. The duration of that state, T_2, is given by

$$T_2 = -(\alpha_m + 2\beta_m + \alpha_h)^{-1}\log_e r_2. \qquad (6)$$

At $t = T_2$, the channel jumps either to [1], [2'], or [3]. The probability of jumping to [1] is $2\beta_m/(\alpha_m + 2\beta_m + \alpha_h)$; the probability of jumping to [2'] is a $\alpha_h/(\alpha_m + 2\beta_m + \alpha_h)$; and the probability of jumping to [3] is $\alpha_m/(\alpha_m + 2\beta_m + \alpha_h)$. A third random number, r_3, is used to determine which of these transitions occurs. The procedure is then continued in a similar manner. The treatment of time varying rate constants for state diagrams is similar to that of Eqs. 2–5. In fact, Eqs. 2–4 are appropriate for the

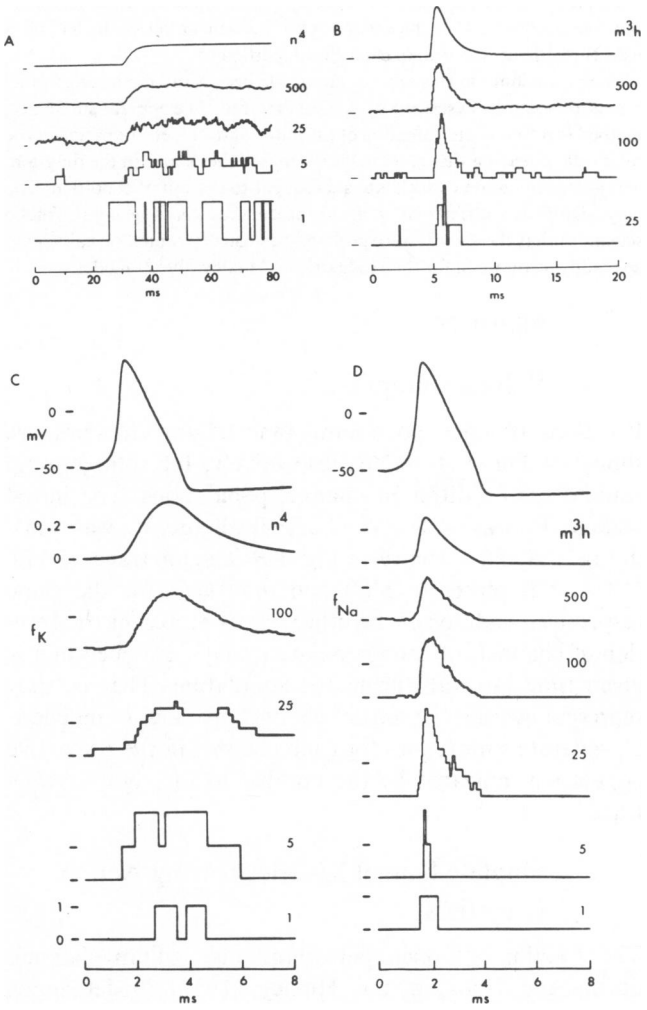

FIGURE 1 Simulations of channel-gating kinetics for a predetermined voltage change. *A*, response of potassium channels to a voltage step with $V_1 = -50$ mV and $V_2 = 0$ mV. Step change occurred at $t_j = 30$ ms. The number of channels is given to the right of each record. The top trace represents the macroscopic parameter $n^4(t)$, where $n(t) = n_2 - (n_1 - n_2)e^{-t/\tau_n}$ with $n_1 = \alpha_n(V_1)/[\alpha_n(V_1) + \beta_n(V_1)]$, $n_2 = \alpha_n(V_2)/[\alpha_n(V_2) + \beta_n(V_2)]$, and $\tau_n = 1/[\alpha_n(V_2) + \beta_n(V_2)]$; $n_1^4(V_1 = -50) = 0.051$; $n_2^4(V_2 = 0) = 0.64$; $\tau_n = 1.78$ ms. The ordinate represents the fraction of open channels. Same scale for all traces. The horizontal line to the left of each of the top four traces represents zero open channels. *B*, response of sodium channels to a voltage step with $V_1 = -50$ mV and $V_2 = -10$ mV. Step change occurred at $t_j = 5$ ms. The number of channels for each simulation is given to the right. The top trace represents the macroscopic parameter $m^3(t)h(t)$ with $m_1^3h_1 = 0.0012$, $m_2^3h_2 = 0.0065$; $\tau_m = 0.35$ ms, $\tau_h = 1.34$ ms. The peak amplitude of $m^3(t)h(t) = 0.103$. Same ordinate scale for the top four traces. *C*, fraction of open potassium channels, f_K, during the Hodgkin and Huxley model (1952) action potential, which is shown in the top trace. Total number of channels given at the right of each simulation. *D*, fraction of open sodium channels, f_{Na}, during the Hodgkin and Huxley model action potential.

simplest possible state diagram consisting of only one closed and one open state. To illustrate the application of this analysis to more complicated diagrams, consider Diagram I in which state [2] is once again the initial condition. Its duration, T, is determined by Eq. 2 with $\beta_x[V(t)]$ replaced by $\{\alpha_m[V(t)] + 2\beta_m[V(t)] + \alpha_h[V(t)]\}$. The transition at $t = T$ is determined as above with the values of the rate constants appropriate for $V(t = T)$. Other aspects of the analysis are treated in a manner similar to that for the simple two-state diagram. The primary difference between the analysis of the Hodgkin and Huxley (1952) model in this and in the previous sections is that the entire gating mechanism for each channel is used throughout rather than each gating particle.

The techniques in this section can be applied to any model of channel gating that can be described by a state diagram. The general simulation method involves a determination of the initial state, a determination of the total rate of leaving that state to one or more other states in the diagram, and a determination of the state subsequent to the initial condition. The only significant difference in these procedures for a general kinetic scheme is that the steady-state probabilities usually cannot be caluclated as readily as they can for the Hodgkin and Huxley (1952) model.

RESULTS

Voltage Jumps

Fractions of open potassium and sodium channels are shown in Fig. 1 *A* and *B*, respectively, for voltage-jump simulations on different channel populations. The initial voltage, V_1, was -50 mV. The final voltage, V_2, was 0 mV in Fig. 1 *A* and -10 mV in Fig. 1 *B*. The top traces in Fig. 1 *A* and *B* represent $n^4(t)$ and $m^3(t)h(t)$, for the same respective conditions. The other traces represent the fraction of channels of each population that were open in any given time interval during the simulation. That is, they represent averaged results of channel openings of individual, separate simulations for each channel in the respective population indicated by the number to the right of each trace.

Single-Channel Kinetics During Action Potentials

The fractions of open potassium and sodium channels during the Hodgkin and Huxley (1952) model action potential (Methods) are shown in Fig. 1 *C* and *D* for different channel populations. The corresponding values of the macroscopic parameters $n^4(t)$ and $m^3(t)h(t)$ calculated in the standard way (FitzHugh, 1969) are also shown. The traces for each of the populations represent the fraction of open potassium channels, f_K, and open sodium channels, f_{Na}. These results were determined in a manner similar to that used to construct the simulation results in Fig. 1 *A* and *B*.

Membrane Excitability

Action potential responses of three different size membrane patches to a near threshold current stimulus are shown in Fig. 2. A near-threshold pulse, I_{app}, was applied from 1 to 1.5 ms; $I_{app} = 0$ at all other times. The size of the patches used was 1, 0.2, and 0.04 μm^2, left to right in Fig. 2, with C_s, I_{app}, N_K, and N_{Na} all scaled according to area. The

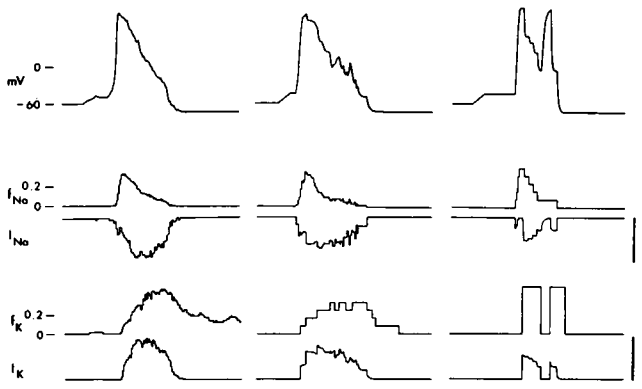

FIGURE 2 Sample action potentials for 1 μm^2 (left), 0.2 μm^2 (middle), and 0.04 μm^2 (right) patches, as described in the text. Fraction of open channels, f_K and f_{Na} and total channel currents, I_K and I_{Na} are given below each action potential. $E_K = -72$ mV, and for these simulations $E_{Na} = 75$ mV rather than 55 mV, which was the value of E_{Na} used in Fig. 1 *C* and *D*. The channel numbers were, left to right, $N_K = 60, 12, 2$; $N_{Na} = 300, 60, 12$; the stimulus amplitude, left to right, was $I_{app} = 0.3125, 0.0625, 0.0125$ pA. Membrane capacitance was determined from $C_M = 1$ $\mu F \cdot cm^{-2}$. Vertical bar represents 12.5, 3, and 0.6 pA, reading from left to right. Horizontal bar represents 1.5 ms for all three results.

fraction of open potassium and sodium channels and the corresponding currents are shown below each action potential.

The variability of the small patch response is illustrated in Fig. 3. The conditions for these simulations were the same as those used for the smallest patch in Fig. 2. The relationship between variability of response and patch size is illustrated in Fig. 4 for response latency. For these results a suprathreshold stimulus was applied from $t = 0$ to $t = 0.5$ ms to membrane patches of area $A = 0.02, 0.04, 0.08, \ldots 2.56$ μm^2 with I_{app}, N_K, N_{Na}, and C_s all scaled according to area. In the smallest patch, $N_K = 1$, $N_{Na} = 5$; in the largest, $N_K = 128$, $N_{Na} = 640$. The latency was taken to be the time

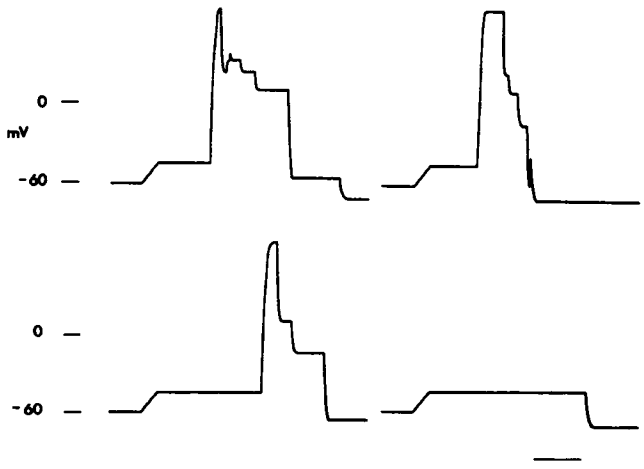

FIGURE 3 Examples of variability of membrane response for a small patch. Same conditions as in the right hand panel of Fig. 2 with different sets of computer generated random numbers. The horizontal bar represents 1.5 ms.

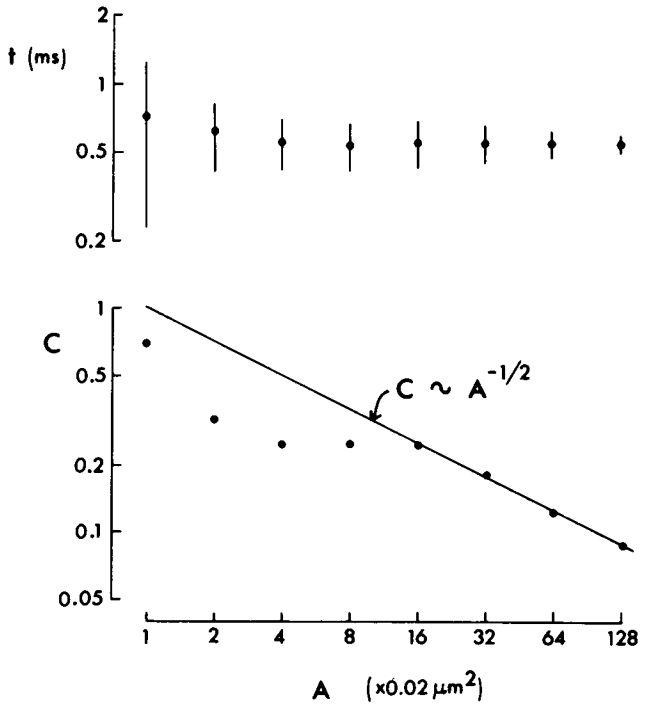

FIGURE 4 Latency fluctuations vs. patch area (A). Each patch was stimulated from $t = 0$ to $t = 0.5$ ms by a current pulse of amplitude equal to 0.02 pA times the number on the abscissa. The total number of simulations for each patch was 10^3. The fraction of simulations that resulted in an action potential was 0.872, 0.912, 0.930, 0.911, 0.944, 0.987, 0.999, 1.000, for patch areas starting with the smallest and progressing to the largest. The mean latency to reach 0 mV for the first time for action potential responses is given in the top part of the figure by the symbol (•). The vertical bar represents the standard deviation from the mean, σ_t. The coefficient of variation, $C = \sigma_t/\bar{t}$ is given in the bottom part of the figure. The solid line represents the relation $C \sim A^{-1/2}$, fitted by eye to the results from the four largest patches.

required for the membrane to reach $V = 0$ mV for the first time. The number of simulations for each patch was 10^3. The mean latency, $\bar{t}$, the standard deviation of the mean, σ_t, and the coefficient of variation, $C = \sigma_t/\bar{t}$, are all shown in Fig. 4.

DISCUSSION

The results in Fig. 1 *A* and *B* illustrate the relationship between open and closed conductance-state lifetimes of a channel and the macroscopic membrane response to a voltage step. Any single channel can give a misleading representation of the macroscopic behavior. For example, the single potassium channel in the simulation represented in the bottom trace of Fig. 1 *A* opened before the voltage jump, which occurred at $t_j = 30$ ms, and it remained open for sometime thereafter. This was not a typical result. Each simulation differed, of course, from all others. The characteristic macroscopic behavior became apparent only when many simulations were averaged together, as the results for 500 channels in Fig. 1 indicate. These results also illustrate the manner in which open and closed conductance state lifetimes of a channel combine to produce the characteristic delay of the macroscopic response. The probability distribution functions for open- and closed-channel states change instantaneously at t_j. That is, the durations of channel states following t_j are determined by the final voltage, V_2. So long as a channel remains in the state at which it found itself at $t = t_j$, it reflects its condition at that time which, in turn, was determined by V_1, the starting potential. Consequently, the macroscopic time constant of membrane response reflects the distribution of the lifetimes of the states of channels at t_1 following the voltage jump.

The results in Fig. 1*C* and *D* illustrate the relationship between the time course of the macroscopic action potential and the underlying potassium and sodium channels. The comparison between the simulations and the macroscopic n^4 and m^3h results in all panels of Fig. 1 provides a self-consistency check on our simulation technique.

The results in Fig. 2 illustrate the relationship between channel openings and closings and the resulting changes in membrane potential as the size of a patch is reduced. The action potential in the left-hand panel for a 1 μm^2 patch is roughly similar in shape to the standard, macroscopic Hodgkin and Huxley (1952) action potential. The general outline of the action potential for a 0.2 μm^2 patch can be discerned, although the event is much noisier. The shape of the voltage waveform for the 0.04 μm^2 patch bears little resemblance to the macroscopic event. The effects of single-channel openings and closings on membrane potential are apparent in this result. The potential changes with an exponential time course following a change in conductance state of a channel with a time constant that is determined by the capacitance of the patch, the number of open channels, and their respective conductances. These results are relevant for small cells, where the input resistance is so high that openings and closings of single channels may have large effects on membrane potential (Hamill et al., 1981).

The results in Fig. 3 indicate that any single voltage response from a small patch cannot be regarded as typical. The response amplitude, latency, and duration are all variable. Moreover, the probability of any depolarization occurring for a near-threshold stimulus is <1, as the result in the lower right-hand panel of Fig. 3 illustrates. Any single response parameter must be represented in a statistical way from a large number of simulations, as demonstrated by the results in Fig. 4, for response latency for patches of varying size. These simulations demonstrate that mean latency is nearly independent of membrane area for the larger patch sizes, whereas the fluctuations in latency are a diminishing function of area with the coefficient of variation, $C \sim A^{-1/2}$ for the four largest patches. The fact that the response latency is independent of A is consistent with the intuitive notion that the mean action potential parameters are independent of size for a space-clamped preparation. For example, a nerve action potential

is theoretically independent of axon diameter in space-clamp conditions, so long as the channel densities are independent of diameter and the current pulse amplitude is scaled according to area. The membrane capacitance, the ionic conductances, g_K, g_{Na}, and g_L all scale in the same way, if the channels are uniformly distributed throughout the axonal membrane with the same distribution for axons of different sizes. Consequently, the membrane area drops out of the equation for the membrane action potential if the stimulus, I_{app}, is scaled appropriately. Experimental preparations may, of course, have a dependence of channel density on axon diameter. The reduction of variability of the action potential parameters as area increases is not surprising, although the specific relationship between variability and patch size is striking. An intuitive basis for the $C \sim A^{-1/2}$ relationship can be obtained from Poisson statistics, since the variance of a Poisson distribution is $\bar{N}^{1/2}$, where $\bar{N}$ is the distribution mean. Consequently, the coefficient of variation for such a process is $\sim\bar{N}^{-1/2}$. Experimental evidence for the $C \sim A^{-1/2}$ result has been reported recently from observations of the beat rate of spontaneously beating clusters containing some number, N ($1 \leq N \leq 125$), of electrically coupled embryonic heart cells (Clay and DeHaan, 1979). Although the mean beat rate was independent of N, the relative beat-to-beat variability of the interbeat interval scaled according to the $C \sim N^{-1/2}$ relation. Further evidence for the general nature of this result has been provided by Enright (1980), who demonstrated with computer simulations that the variability in first passage time to a threshold for some number, N, of coupled, noisy oscillators scales according to $N^{-1/2}$. This reduction of variability with size provides one way in which coupled, noisy cells can produce coherent, or rhythmic, behavior.

The primary purpose of this paper is to describe a method of calculating membrane current or voltage responses at the level of single channels from macroscopic ion conductance equations. We have illustrated the technique with the Hodgkin and Huxley (1952) model of the nerve action potential. This model is known to provide an incomplete representation of macroscopic membrane current measurements from nerve, including squid giant axons for which it was originally designed (Cole and Moore, 1960; Bezanilla and Armstrong, 1977; Shoukimas and French, 1981; Oxford, 1981; Clay and Shlesinger, 1982). Measurements of single channel kinetics in excitable membranes also illustrate the inadequacies of the model (Conti and Neher, 1980; Sigworth and Neher, 1980). In particular, the measurements of Conti and Neher (1980) suggest that a channel occasionally flickers rapidly between its open state and one of its closed states during any individual open-state lifetime. Alternative models that demonstrate flickering behavior have been analyzed recently by Colquhoun and Hawkes (1981). Simulations similar to the ones we have performed could be carried out for these or any other models, as described above (Methods). Our primary purpose in using the Hodgkin and Huxley (1952) model was to illustrate a novel stimulation technique. Other investigators have presented simulations for voltage jumps or steady-state voltage-clamp conditions (Colquhoun and Hawkes, 1977; Baumann and Easton, 1980; Lecar and Sachs, 1981). These authors did not present results for conditions in which either the rate constants for transitions between states are effectively time dependent or the membrane is unclamped. As we have shown, the solution to these problems can be generalized from our treatment of single channel kinetics in steady-state voltage-clamp conditions.

Analysis of the relationship between single channel kinetics and membrane excitability effectively turns the noise problem back to its origins, as Sigworth (1980) has recently noted. The original observations by Blair and Erlanger (1932), Pecher (1939), and Verveen (1961) of fluctuations in excitability in response to a constant near-threshold stimulus provided at least some of the original motivation for membrane noise measurements. Earlier theoretical treatments of fluctuations of excitability consisted of analysis of macroscopic conductance equations to which idealized, model noise sources were added (Lecar and Nossal, 1971 *a*, *b*; Clay, 1976, 1977). Because the principle noise source in excitable membranes can now be assigned to the single-channel open-close process, the problem of fluctuations of excitability can be treated directly by assigning noise properties to the conductance parameters in the microscopic, single-channel domain.

We gratefully acknowledge M. F. Shlesinger and A. Mauro for stimulating discussions concerning this work.

Supported in part by National Institutes of Health grant 1-PO1-HL27385 to Dr. DeFelice.

Received for publication 1 July 1982 and in final form 11 January 1983.

REFERENCES

Armstrong, C. M., and F. Bezanilla. 1977. Inactivation of the sodium channel. II. Gating current experiments. *J. Gen. Physiol.* 70:567–590.

Armstrong, C. M., and W. F. Gilly. 1979. Fast and slow steps in the activation of sodium channels. *J. Gen. Physiol.* 74:691–711.

Baumann, G., and G. S. Easton. 1980. Micro- and macrokinetic behavior of the subunit gating channel. *J. Membr. Biol.* 52:237–243.

Bezanilla, F., and C. M. Armstrong. 1977. Inactivation of the sodium channel. I. Sodium current experiments. *J. Gen. Physiol.* 70:549–566.

Blair, E. A., and J. Erlanger. 1932. Responses of axons to brief shocks. *Proc. Soc. Exp. Biol. Med.* 29:926–927.

Clay, J. R. 1976. A stochastic analysis of the graded excitatory response of nerve membrane. *J. Theor. Biol.* 59:141–158.

Clay, J. R. 1977. Monte Carlo simulation of membrane noise: an analysis of fluctuations in graded excitation of nerve membrane. *J. Theor. Biol.* 64:671–680.

Clay, J. R., and R. L. DeHaan. 1979. Fluctuations in interbeat interval in rhythmic heart-cell clusters. Role of membrane voltage noise. *Biophys. J.* 28:377–390.

Clay, J. R., and M. F. Shlesinger. 1982. Delayed kinetics of squid axon

potassium channels do not always superpose after time translation. *Biophys. J.* 37:677–680.

Cole, K. S., and J. W. Moore. 1960. Potassium ion current in the squid giant axon: dynamic characteristic. *Biophys. J.* 1:1–14.

Colquhoun, D., and A. G. Hawkes. 1977. Relaxation and fluctuations of membrane currents that flow through drug-operated channels. *Proc. R. Soc. Lond. B. Biol. Sci.* 199:231–262.

Colquhoun, D., and A. G. Hawkes. 1981. On the stochastic properties of single ion channels. *Proc. R. Soc. Lond. B. Biol. Sci.* 211:205–235.

Conti, F., L. J. DeFelice, and E. Wanke. 1975. Potassium and sodium ion current noise in the membrane of the squid giant axon. *J. Physiol. (Lond.)*. 248:45–82.

Conti, F., and E. Neher. 1980. Single channel records of K^+ currents in squid axons. *Nature (Lond.)*. 285:140–143.

Enright, J. T. 1980. Temporal precision in circadian systems: a reliable clock from unreliable components? *Science (Wash., DC)*. 209:1542–1545.

Feller, W. 1971. An Introduction to Probability Theory and Its Applications. John Wiley & Sons, Inc. New York. 2:8–9.

FitzHugh, R. 1965. A kinetic model of the conductance change in nerve membrane. *J. Cell. Comp. Physiol.* 66:111–118.

FitzHugh, R. 1969. Mathematical models of excitation and propagation in nerve. *In* Bioelectronics. H. P. Schwan, editor. McGraw-Hill, Inc. New York. 1–85.

Gilly, W. F., and C. M. Armstrong. 1982. Divalent cations and the activation kinetics of potassium channels in squid giant axons. *J. Gen. Physiol.* 79:965–996.

Hamill, O. P., A. Marty, E. Neher, B. Sakmann, and F. J. Sigworth. 1981. Improved patch clamp techniques for high resolution current recording from cells and cell free membrane patches. *Pflügers Archiv. Gesamte Physiol. Menschen Tiere.* 391:85–100.

Hill, T. L., and Y. Chen. 1972. On the theory of ion transport across the nerve membrane.IV. Noise from the open-close kinetics of K^+ channels. *Biophys. J.* 12:948–959.

Hodgkin, A. L., and A. F. Huxley. 1952. A quantitative description of membrane current and its application to conduction and excitation in nerve. *J. Physiol. (Lond.)*. 117:500–544.

Karlin, S., and H. M. Taylor. 1975. A First Course in Stochastic Processes. Academic Press, Inc. New York. 155.

Lecar, H., and R. Nossal. 1971 *a*. Theory of threshold fluctuations in nerves. I. Relationships between electrical noise and fluctuations in axon firing. *Biophys. J.* 11:1048–1067.

Lecar, H., and R. Nossal. 1971 *b*. Theory of threshold fluctuations in nerves. II. Analysis of various sources of membrane noise. *Biophys. J.* 11:1068–1084.

Lecar, H., and F. Sachs. 1981. Membrane noise analysis. *In* Excitable Cells in Tissue Culture. P. G. Nelson and M. Lieberman, editors. Plenum Publishing Corp. New York. 137–172.

Moore, J. W., and F. Ramon. 1974. On numerical integration of the Hodgkin and Huxley equations for a membrane action potential. *J. Theor. Biol.* 45:249–273.

Neher, E., and C. F. Stevens. 1977. Conductance fluctuations and ionic pores in membranes. *Annu. Rev. Biophys. Bioeng.* 6:345–381.

Oxford, G. S. 1981. Some kinetic and steady-state properties of sodium channels after removal of inactivation. *J. Gen. Physiol.* 77:1–22.

Pecher, C. 1939. La fluctuation d'excitabilité de la fibre nerveuse. *Arch. Int. Physiol.* 49:129–152.

Rush, S., and H. Larsen. 1978. A practical algorithm for solving dynamic membrane equations. *IEEE (Inst. Electr. Electron. Eng.) Trans. Biomed. Eng.* 25:389–392.

Shoukimas, J. J., and R. J. French. 1981. Incomplete inactivation of sodium currents in nonperfused squid axons. *Biophys. J.* 32:857–862.

Sigworth, F. J. 1980. The variance of sodium current fluctuations at the node of Ranvier. *J. Physiol. (Lond.)*. 307:97–129.

Sigworth, F. J., and E. Neher. 1980. Single Na^+ channel currents observed in cultured rat muscle cells. *Nature (Lond.)*. 287:447–449.

Stevens, C. F. 1972. Inferences about membrane properties from electrical noise measurements. *Biophys. J.* 12:1028–1047.

Verveen, A. A. 1961. Fluctuation in Excitability. Eindhorensche, Drukkerij, Amsterdam. 1–76.